Formability analysis of aluminum alloys through deep drawing process

U Pranavi[1], Perumalla Janaki Ramulu[2#], Ch Chandramouli1, Dasari Govardhan[3], PVS.Ram Prasad[4]

[1]Department of Mechanical Engineering, Vardhaman College of Engineering, Hyderbad-501218, India; upranavi908@gmail.com; moulimailme@gmail.com.

[2]School of Mechancial, Chemical and Materials Engineering. Adama Science and Technology University, Ethiopia, perumalla.janaki@astu.edu.et* #corresponding author

[3]Department of Mechanical Engineering, Visvesvaraya College of Engineering and Technology,Hyderabad, India; dgvardhan@gmail.com.

[4]Department of Mechanical Engineering, Anurag College of Enginnering, Ghatkesar, Hyderabad, India; pvsramprasad@gmail.com.

Abstract. Deep drawing process is a significant metal forming process used in the sheet metal forming operations. From this process complex shapes can be manufactured with fewer defects. Deep drawing process has different effectible process parameters from which an optimum level of parameters should be identified so that an efficient final product with required mechanical properties will be obtained. The present work is to evaluate the formability of Aluminum alloy sheets using deep drawing process. In which effects of punch radius, lubricating conditions, die radius, and blank holding forces on deep drawing process observed for AA 6061 aluminum alloy sheet of 2 mm thickness. The numerical simulations are performed for deep drawing of square cups using three levels of aforesaid parameters like lubricating conditions and blank holding forces and two levels of punch radii and die radii. For numerical simulation a commercial FEM code is used in which Hollomon's power law and Hill's 1948 yield criterions are implemented. The deep drawing setup used in the FEM code is modeled using a CAD tool by considering the modeling requirements from the literature. Two different strain paths (150x150mm and 200x200mm) are simulated. Punch forces, thickness distributions and dome heights are evaluated for all the conditions. In addition failure initiation and propagation is also observed. From the results, by increasing the coefficient of friction and blank holding force, punch force, thickness distribution and dome height variations are observed. The comparison has done and the optimistic parameters were suggested from the results. From this work one can predict the formability for different strain paths without experimentation.

1. Introduction

Deep drawing is a manufacturing process that is used extensively in the forming of sheet metal into cup or box like structures under tensile and compressive conditions, without altering the sheet thickness. Pots and pans for cooking, containers, sinks, automobile parts, such as panels and gas tanks, are among a few of the applications manufactured by sheet metal deep drawing. The formability of a blank during the deep drawing is depends on the process parameters such as blank holder force, lubrication, punch and die radius, die–punch clearance, in addition to mechanical properties and thickness of the sheet metal and part's geometry. Many studies have been carried out on numerical simulations of deep drawing process. For example, Meinders [1] investigated the behavior of tailored blanks during deep drawing using the finite element code. They simulated the deep drawing of two products using Tailored Blanks and observed that the experimental and simulation results were correlated satisfactory. Takuda [2] simulated the deformation behavior and the temperature change in deep drawing of an aluminum alloy sheet and successfully predicted the forming limit and necking site by comparing the numerical results with experimental results. Yoshihara [3] investigated deep-drawing process of a circular cup using magnesium alloy material and found that wall thickness of the drawn cup depends on the initial BHF value. Padmanabhan [4] evaluated the orientation of blank sheets rolling direction during deep drawing process and the effect of anisotropy in the tailor-welded blank and noticed that the punch force for deep drawing increases with anisotropy in the blank sheets.

Jawad [5] studied the effects of varying punch nose radius used in the deep drawing process by carrying out the numerical simulation process in commercially finite element program code. Compared the experimental work with numerical results, it was concluded that large frictional force is applied to the metal by the edge of the punch, but not by its flat section. Also the work required to form a part with large nose radius is more than that required to form a part with small punch nose radius. Hama [6] studied the tool modeling accuracy on a square-cup deep-drawing operation using finite element simulation and quadratic parametric surfaces proposed by Nagata patch. It was presented that the total number of tool elements can be reduced to about 10% of the polyhedral model. Rodrigues [7] determined a multi-step analysis for admissible blank-holder forces in deep drawing process for stamping friction stir welded tailored blanks and the formability behavior of similar and dissimilar combinations of AA 5182-H111 and AA 6016-T4 aluminum alloys were previewed. Using the theoretical stress based criteria; analytical FLDs were plotted and compared their formability limits with the principal strains in the cup walls obtained by the numerical simulation of the deep-drawing tests, thereby concluded that the procedure can be used to determine the maximum BHF for deep drawing different TWBs. Arab [8] examined the deep drawing process of axi-symmetric cylindrical cup with anisotropic Hill's non-yield criterion and rigid visco-plastic finite element method. The experimental validation of the numerical prediction was found to be satisfactory for thickness distributions and deformation stages on the sheet.

From the above studies, it is observed that the essentiality of the proper selection of process parameters to the deep drawing process is very crucial. The process parameters selection is also depends on the base material. It is essential to study the process numerically before experimentation. The objective of the present work is to identify the desired lubrication and blank holding force for AA 6061 alloy during the deep drawing process.

2. Methodology

2.1. Base material properties and process parameters

For conducting simulation, the material and process parameters that affect the deep drawing behavior were identified from available literature. The mechanical and forming properties of aluminum base metal used in FE simulations are shown in Table 1. The effectible parameters of deep drawing process parameters like coefficient of friction and blank holding force were considered for simulation. These two parameters were varied in three levels as shown in Table 2.

Table 1. Mechanical properties of base material AA 6061-T6 [9]

Material	E (GPa)	γ	σ (MPa)	K (MPa)	n	R_0	R_{45}	R_{90}	t (mm)
AA 6061	66	0.33	269	419	0.1	0.79	0.95	0.85	2

Table 2. Three levels Process parameters and considered value

Process parameters	Value
Coefficient of Friction (μ)	0.1
	0.15
	0.2
Blank holding force (BHF) (kN)	10
	20
	15

2.2. Modeling and Simulation of Deep drawing process

In CAD modeling, the tools required for the test, blank, punch, blank holder and die were generated as shown in Figure 1. Simulations of deep drawing process were simulated using a finite element code. The sheet comprised of quadrilateral shell elements with five through thickness integration points of Belytschko-Tsay formulation. The strain hardening law and the plasticity model considered were the Hollomon's power law ($\sigma = K\varepsilon^n$; where σ-true yield strength; K-strength coefficient; ε-true strain; n-strain hardening coefficient) and the Hill's 1948 isotropic hardening yield criterion respectively. Two base material sheets each of size 150x150mm and 200x200mm were taken for all the conditions. A uniform meshing of size 1mm was used throughout the simulations. The yield strength was kept constant and the friction coefficients taken were 0.1, 0.15 and 0.2. The blank holder forces considered were 10kN, 15kN and 20kN. Downward stroke to the punch is given with a velocity of 10mm/min and a total of 18 simulations were performed by varying the coefficient friction and blank holder force. From the simulation results the thickness distribution, punch force, and dome height were evaluated.

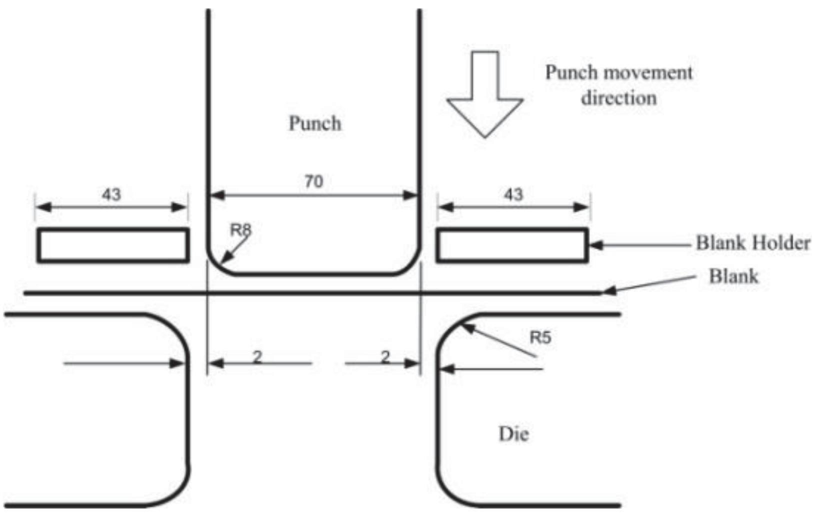

Figure 1. Deep drawing set for Simulations

3. Results

3.1. Punch Force Evaluation

The variation of punch force for two different strain paths, 150x150mm and 200x200mm were observed graphically. The analysis was carried out by comparing the effect of varying blank holding forces at constant lubrication condition. The blank holding forces considered were 10kN, 15kN and 20kN. The lubrication conditions used for examining were the coefficient of friction values 0.1, 0.15 and 0.2. The graphs were compared at two different punch radii and die radii. The evaluation of the punch force was as follows.

3.2. Punch Radius 8mm and Die Radius 5mm

Initially the evaluation was performed for the simulations where the punch radius was 8mm and die radius was 5mm. The distinction in punch force by varying blank holding force can be viewed from the Figures 2, and 3 for the strain path 150x150mm and from Figures 5, 6 and 7 for the strain path 200x200mm. The comparison was done by considering punch force along the ordinate in kilo newtons and the displacement of the blank at the centre along abscissa in millimeters of the coordinated system.

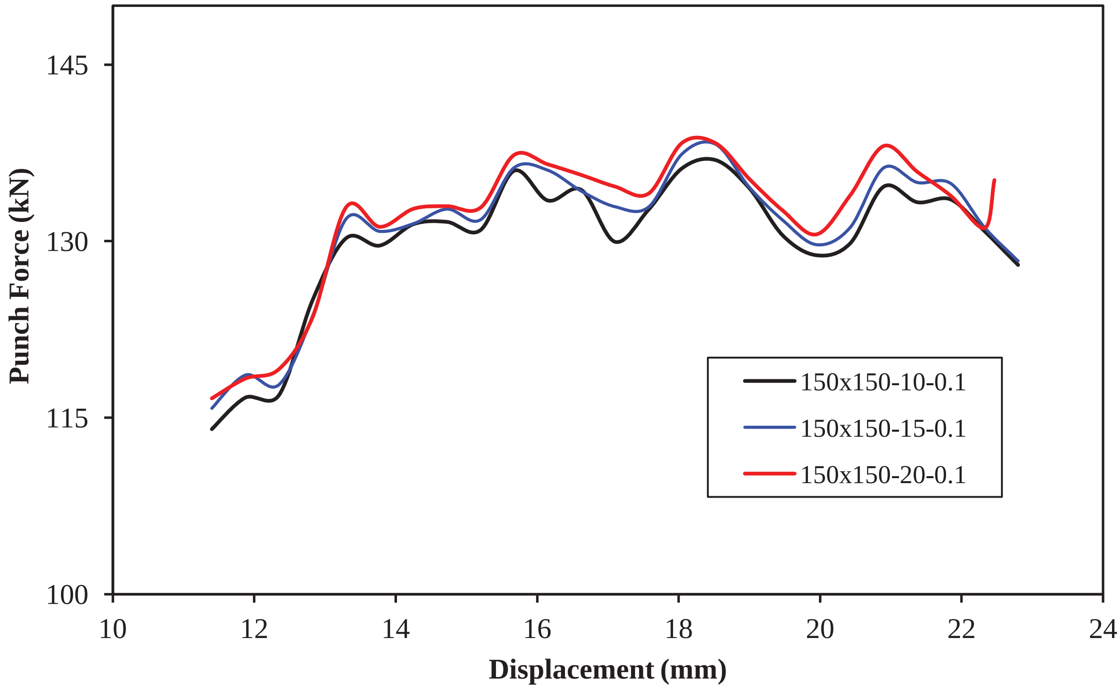

Figure 2. Punch force comparison at constant frictional coefficient (0.1) and at different blanks holding forces for the blank of size 150x150 mm.

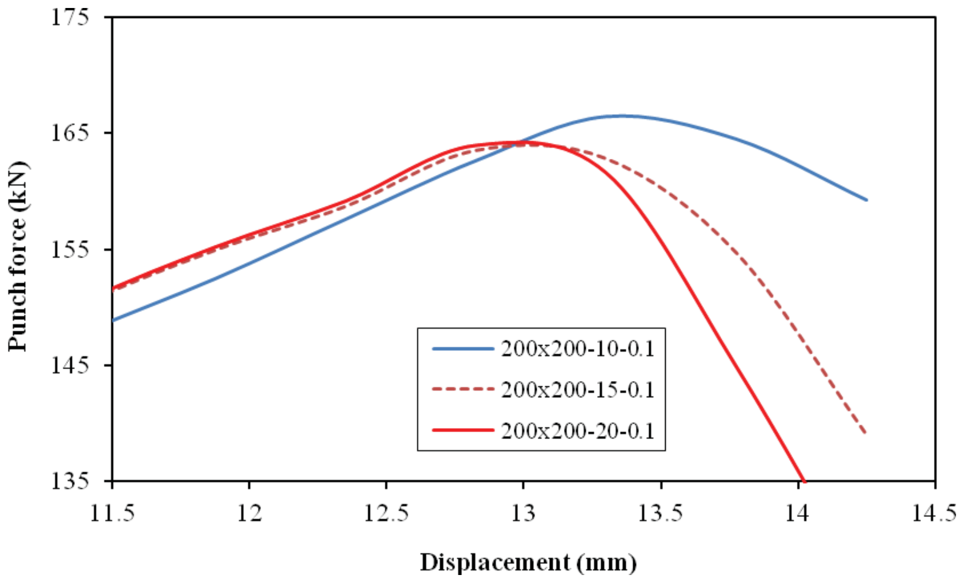

Figure 3. Punch force comparison at constant frictional coefficient (0.1) and at different blanks holding forces for the blank of size 200x200 mm.

Table 3. Punch force variation at constant lubricating conditions and varying blank holder force.

Strain path	Lubrication Condition	Blank holder force (kN)	Maximum punch force (kN)
150x150 mm	0.1	10	136.9
		15	138.2
		20	138.4
	0.15	10	143.8
		15	145.3
		20	146.6
	0.2	10	150.8
		15	151.5
		20	152.5
200x200 mm	0.1	10	166.5
		15	163.5
		20	163.9
	0.15	10	155.3
		15	153.5
		20	150.1
	0.2	10	147.8
		15	145.1
		20	143.8

The variations in the punch force from the simulation results were shown in the above Table 3 and the reasons for the variations in the above values were explained further.

Blank holder forces 10kN, 15kN and 20kN with coefficient of friction 0.1, 0.15 and 0.2 were used in simulations for understanding the formability of AA6061 Aluminum alloy material. A 150x150mm blank with 2 mm thickness was developed and a total of nine simulations were observed for deep drawing of square cup (Table 3). From the simulations, it was found that maximum punch force was 152kN and minimum was 136kN. The punch force analysis reveals that with increase in the blank holder force at constant lubrication condition, the punch force increases. The 200x200mm blank of 2mm thickness was also developed and nine simulations were observed for the square cup (Table 3). The punch force analysis reveals that as the blank holder force increases, the punch force decreases. Table 1 illustrates that for 200x200mm strain path the punch force varies between 166kN and 143kN. Simulation results of both the strain paths for 10kN, 15kN and 20kN blank holder forces reveals that as the size of the blank increases the punch force increases for coefficient of friction 0.1 and 0.15 (Table 3). But for the condition where the coefficient of friction is 0.2, the punch force decreases with increase in the blank holder force.

3.3. Evaluation of dome height and failure location

The dome height was the progression at which the initial necking takes place for the sheet metal blank. The necking criterion was observed based on the thickness gradient necking criterion (Nandedkar, (2000)) in which the ratio of the two consequent elements must be less than or equal to 0.92.

3.4 Punch Radius 8mm and Die Radius 5mm

The Dome height of AA 6061 Aluminum alloy was evaluated for punch radius 8mm and die radius 5mm by considering the blank holder forces as 10, 15 and 20kN and coefficient of friction as 0.1, 0.15 and 0.2 for the strain paths 150x150mm and 200x200mm. The failure propagation was observed around the side walls of the blank and the failure initiation in all the simulations was noticed at the side walls of the blank. The state of initial failure propagation and the dome height at initial necking for the simulations were tabulated in the Table 4.

Table 4. Dome heights and initial failure propagation from simulations of punch radius 8mm and die radius 5mm

S. No	Condition	Dome Height (mm) (based on TGNC)	Initial failure location Progression (mm)
1	150x150-10kN-0.10	23.0	18.52
2	150x150-10kN-0.15	18.0	18.05
3	150x150-10kN-0.20	14.0	18.05
4	150x150-15kN-0.10	18.0	18.53
5	150x150-15kN-0.15	16.0	18.05
6	150x150-15kN-0.20	14.0	18.05
7	150x150-20kN-0.10	18.0	18.05
8	150x150-20kN-0.15	18.0	18.52
9	150x150-20kN-0.20	13.0	18.05
10	200x200-10kN-0.10	13.0	13.30
11	200x200-10kN-0.15	12.0	11.87
12	200x200-10kN-0.20	11.0	10.92
13	200x200-15kN-0.10	13.0	12.82
14	200x200-15kN-0.15	12.0	11.40
15	200x200-15kN-0.20	11.0	10.92
16	200x200-20kN-0.10	13.0	12.82
17	200x200-20kN-0.15	12.0	11.40
18	200x200-20kN-0.20	11.0	10.92

IOP Conf. Series: Materials Science and Engineering **149** (2016) 012025 doi:10.1088/1757-899X/149/1/012025

From the Table 3 it was observed that maximum dome height was 23mm for the strain path condition 150x150mm with coefficient of friction 0.1 and 10kN blank holding force. The dome height decreased as the coefficient of friction varied to 0.15 and 0.2 with constant blank holding force. The failure initiation and the dome height for the strain path condition 150x150mm were shown in the Figures 4 and 5 respectively.

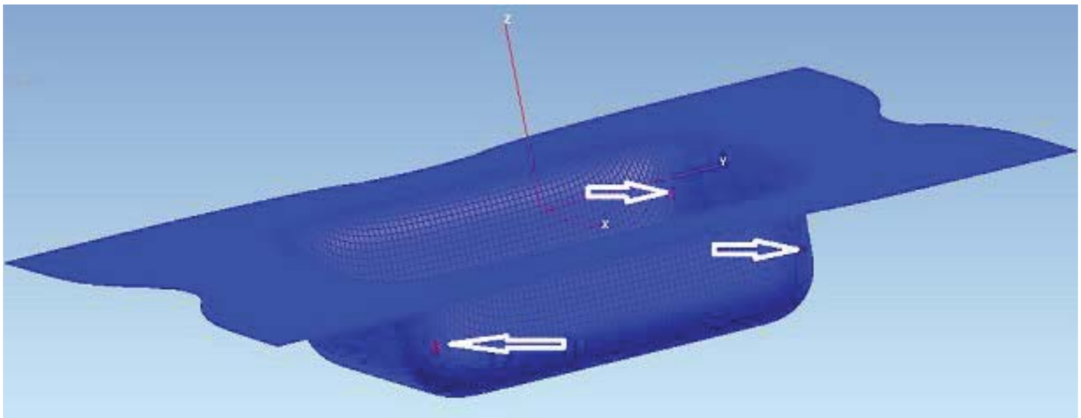

Figure 4. Failure initiation in 150x150mm strain path

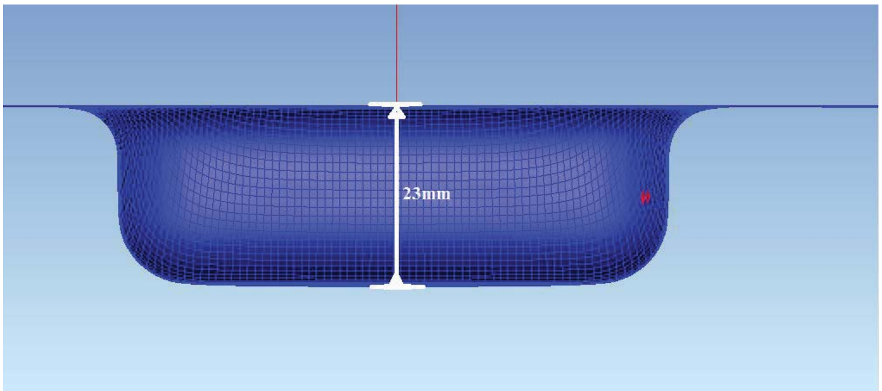

Figure 5. Maximum Dome height for the strain path 150x150mm

In 200x200mm strain path, maximum dome height was noted as 13mm for the coefficient of friction 0.1 as the blank holding force increased from 10kN to 20kN. The failure initiation and the dome height for the strain path condition 200x200 mm were shown in the Figures 6 and 7 respectively.

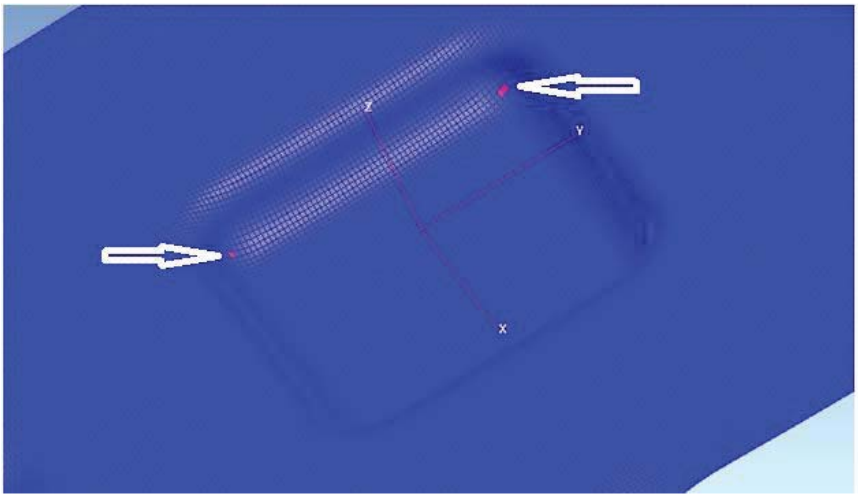

Figure 6. Failure initiation in 200x200mm strain path

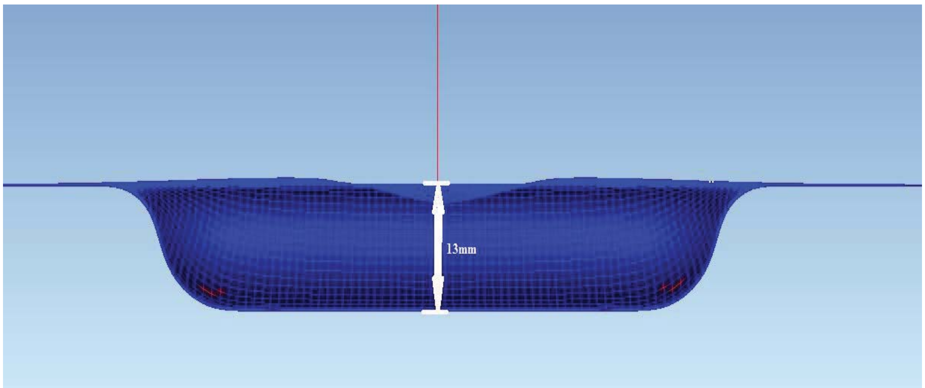

Figure 7. Dome height in 200x200mm strain path

The failure propagation in the strain path 150x150mm was shown in Figures 8 and the failure propagation for 200x200mm strain path was shown in Figure 9.

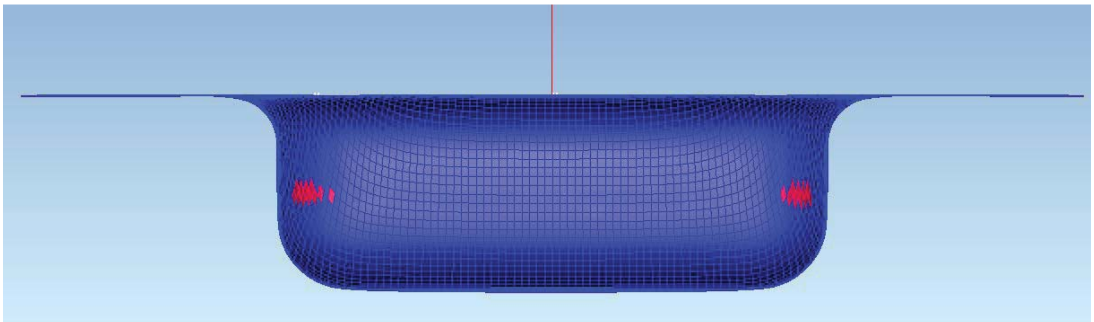

Figure 8. Failure propagation for the strain path 150x150mm

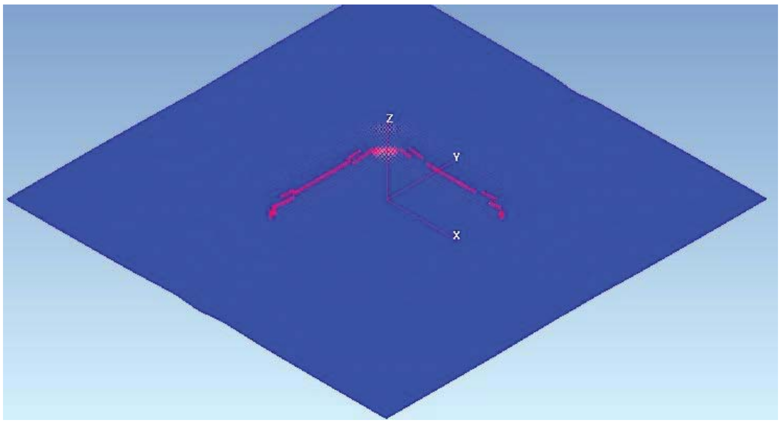

Figure 9. Failure propagation for the strain path 200x200mm

In this study, the dome height ranges from 23mm to 13mm for 150x150mm strain path for three distinct values of blank holder forces and friction coefficients (Table 4). The dome height for 200x200mm strain path ranges between 13mm and 11mm. The dome height decreased as the strain path increased.

Deep drawing process for 10kN, 15kN and 20kN blank holder forces was equal up to 18 mm punch progression (Table 4) for 150x150mm blank sheet and vary between 10mm to 13mm (Table 4) for 200x200mm blank sheet. The failure initiation in the square cup was observed at same point of progression value. The failure propagation was observed at the side walls of the blank in the later progressions. It was observed that the dome height decreases as coefficient of friction varies from 0.1 to 0.2 for the strain path 150x150mm (Table 4). Also the dome height decreases as the blank holder force increases. The dome height decreased as the coefficient of friction varied from 0.1 to 0.2 for the strain path 200x200mm. It remained same with the increase in the blank holding force. The initial failure progression value varied between 13mm and 10mm indicating very slight deviation in the failure point of the square cup. The material flow rate was improved by reducing the sheet metal blank size and simulations are performed. The results (refer to Table 3) show that smaller sheet metal blank model improves material flow. Failure initiation was improved and the increase in the punch force for blank was also prevented for smaller blank with increase in the blank holder force.

Conclusions

1. The effect of the punch force during the simulation is evaluated. It is observed that by increasing the coefficient of friction punch force is improved for 150x150mm strain path. For 200x200mm strain path with the increase in the coefficient of friction, the punch force decreased.
2. It shows that the strain path with comparatively small size experiences increase in the punch force with increase in the coefficient of friction.
3. The effect of the blank holding force during the simulation is observed. It is noted that by increasing the coefficient of friction the blank holding force is improved for 150x150mm strain path. For 200x200mm strain path with the increase in the coefficient of friction, the punch force decreased.
4. The failure initiation in the strain paths of 150x150mm and 200x200mm are same irrespective of changed parameters during simulation process.
5. Maximum dome height is noted is 23mm for the strain path 150x150mm and as 11mm for 200x200mm strain path. The dome height decreases with increase in the strain path. It is also observed that the dome height increased with decrease in the punch force.

References

[1] Meinders T, Vanden Berg A, and Huetink J 2000 *Deep drawing simulations of tailored blanks and experimental verification*, Journal of Materials Processing Technology, 103, pp. 65-73.

[2] Takuda H, Mori K, Masuda I, Abe Y, Matsuo M 2002 *Finite element simulation of warm deep drawing of aluminum alloy sheet when accounting for heat conduction*, Journal of Materials Processing Technology, 120, pp. 412–418.

[3] Yoshihara S, Ken ichi Manabe, Hisashi Nishimura 2005 *Effect of blank holder force control in deep drawing process of magnesium alloy sheet*, Journal of Materials Processing Technology, 170, pp. 579–585.

[4] Padmanabhan R, Baptista A.J, Oliveira M, Menezes L.F. 2007 *Effect of anisotropy on the deep-drawing of mild steel and dual-phase steel tailor-welded blanks*, Journal of Materials Processing Technology, 184, pp. 288–293.

[5] Waleed K Jawad, Jamal H Mohamed 2008 *Studying the effect of punch nose radius on deep drawing operation,* Eng. And Tech., 26, pp. 55-73.

[6] Takayuki Hama, Masato Takamura, Akitake Makinouchi, Cristian Teodosiu and Hirohiko 2008 *Effect of Tool-Modeling Accuracy on Square-Cup Deep Drawing Simulation,* Materials Transactions, 49, pp. 278 - 283.

[7] Rodrigues D. M, Leitao C, Menezes, L F 2010 *A Multi-Step Analysis for Determining Admissible Blank-Holder Forces in Deep-Drawing Operations*, Materials and Design, 31, pp. 1475-1484.

[8] Najmeddin Arab 2013 *Experimental and Cylindrical Simulation Analysis of Deep Cylindrical Simulation Analysis of Deep Cylindrical Cup Process*, Merit Research Journal of Petroleum, Geology and Mining, 1(1), pp. 001-008.

[9] Janaki Ramulu P, Ganesh Narayanan R, Kailas S V, Jayachandra Reddy 2013 *Internal defect and process parameter analysis during friction stir welding of Al 6061 sheets* International Journal of Advanced Manufacturing Technology, 65, pp. 1515-1528.

[10] Nandedkar V. M. 2000 *Formability studies on a deep drawing quality steel*, PhD Thesis. IIT Bombay, India.